

EFFECTS OF HEAT TRANSFER ON MHD FLOW OF BLOOD THROUGH AN INCLINED POROUS ARTERY WITH STENOSIS HAVING VARIABLE VISCOSITY

BHAVYA TRIPATHI AND BHUPENDRA KUMAR SHARMA

ABSTRACT

In this paper, effects of heat transfer on the blood flow through a stenosed, inclined non-tapered porous artery subject to the action of external magnetic field is investigated. Viscosity is assumed as variable viscosity with variable Hematocrit throughout the region of the artery. Governing equations have been modeled by taking blood as incompressible magnetohydrodynamic (MHD) Newtonian fluid. Energy equation is formulated by taking an extra factor of the heat source in its equation. The nonlinear momentum equations are simplified under the assumption of mild stenosis. Homotopy perturbation method (HPM) is used to solve nonlinear equations of velocity and temperature profiles. Effects of porosity parameter (Z), applied magnetic field parameter (M), variable hematocrit parameter (H_r), Brinkman number (Br), heat source parameter (Q) and the Grashof number (Gr) on velocity and temperature profiles are discussed graphically.

Keywords: Newtonian Fluid, Incompressible fluid, Stenosis, Magneto hydro dynamical fluid (MHD), Inclined Porous Artery, Variable Viscosity, Homotopy Perturbation Method.

1. INTRODUCTION

Nowadays in the industrialized world blood flow in our body through arteries is a major cause of health risks. In circulatory system of the human body highly, oxygenated blood and nutrients deliver from heart to each cell of the body through arteries. So deposition of matter in an artery affects the work function of the artery. Abnormal elongation of arterial thickness is the first smallest step in the formation of atherosclerosis.

The accumulation of substances in arteries is known as stenosis and presence of the stenosis in the artery changes its flow behavior and hemodynamic conditions that exist in the artery before catheterization [8, 30]. A well-known disease angina is a cause of stenosis in the coronary artery. The heart receives its own supply of blood from the coronary arteries [3]. In the case of fatty deposition like when cholesterol deposits on an artery wall and when hard plaques form, the coronary artery becomes narrow. These plaques narrow the arteries or may break off and form blood clots that block the arteries. At that time, it is increasingly difficult for oxygenated rich blood to reach the heart muscle because of the narrowing of the artery [26, 32]. At the larger scale of artery blockage causes heart attacks. So recently it has gained a serious attention of researchers, physiologists and clinical persons to study the blood flow through arteries. Excellent works in the context of arterial blood flow in the presence of stenosis has been reported by Lipscomb and Hooten [13], Mekheimer and Kot [18] and Nadeem *et al.* [24].

The erythrocyte (Red blood cell) is a highly specialized cell present in the blood. Since erythrocyte has small negative charge, an applied magnetic field can influence the motion of erythrocyte. A new area of research in fluid dynamics is biomagnetic fluid dynamics (BFD) and it is about to study the dynamics of biological fluids in the presence of magnetic field. MHD differs from BFD in that it deals with magnetic

Date: August 30, 2022.

properties of electrically conducting fluids and the flow is not affected by the magnetization or polarization of the fluid in the magnetic field. MHD has numerous proposed applications in bioengineering and medical sciences [15]. The blood flow in our body through arteries with stenosis under the influence of magnetic field is studied by Tzirtzilakis [37]. Influence of radially varying MHD on the peristaltic flow in an annulus with heat and mass transfer studied by Nadeem and Akbar [23]. A model reported by Shashi Sharma *et al.* [34] which shows the effect of the external uniform magnetic field on flow parameters of both blood and magnetic particles using magnetohydrodynamics(MHD) approach. Sharma *et al.* [33] with Joule effect numerically investigated the heat and mass transfer effect in magneto-biofluid through a non-darcian porous medium. Magnetic particle capture for biomagnetic fluid flow in stenosed aortic is discussed by Abdulla *et al.* [1], Bose and Banerjee [4]. Misra *et al.* [19] proposed a model of blood flow in a porous vessel having double stenoses in the presence of an external magnetic field. Flow of an electrically conducting fluid characterizing blood through the arteries having irregularly shaped multi-stenoses in the environment of a uniform transverse magnetic field is analyzed by Mustapha *et al.* [20] and by Mekheimer [17]. Ikbal *et al.* [10] investigated a model for non-Newtonian flow of blood through a stenosed artery in the presence of a transverse magnetic field. In which blood is characterized by a generalized Power law model. Above mentioned research has been done for showing the magnetic field effects on blood flow but their studies are restricted in consideration of variable viscosity.

However, In real physiological system, the blood viscosity is not constant, it may vary either in hematocrit ratio or depends on temperature and pressure [35]. Layek *et al.* [12] analyzed functional dependence of blood viscosity on hematocrit, viscosity increases with the increasing value of the hematocrit parameter. In the same direction Sinha and Misra [36] presented a model of dually stenosed artery with hematocrit-dependent viscosity. The influence of heat transfer with temperature dependent viscosity is analyzed by Massoudi and Christie [16], Pantokratoras [27], Nadeem and Akbar [21]. In the same direction effects of temperature dependent viscosity with thermal conductivity on heat transfer and fluid flow are analyzed by Umavathi *et al.* [38], Makinde and Onyejekwe [14]. Nadeem *et al.* [22, 25] proposed model for peristaltic flow when the viscosity is not constant.

In the case of stenosis when cholesterol deposits on artery wall and artery-clogging blood clots in the lumen of the coronary artery this stage in the blood flow can be considered as equivalent to a fictitious porous medium [6]. El-Shahed [6] reported a model for pulsatile flow of blood through a stenosed porous artery under the periodic body acceleration. Akbarzadeh [2] numerically investigated the effect of periodic body acceleration and periodic body pressure gradient on MHD blood flow through a porous artery. Kumar *et al.* [11] presented computational techniques for blood flow in arteries with porous effects. Bhatti and Abbas presented a model for Jeffrey fluid which shows the effects of slip and MHD on peristaltic blood flow through a porous medium. Petrofsky *et al.* [28] examined the skin blood flow response to the effect of moisture content of the heat source through data. Prakash *et al.* [29] formulated a model for bifurcated arteries to study the effects of heat source on MHD blood flow. In the same direction Eldesoky [7] studied the effects of heat source on MHD blood flow which passes through a parallel plate channel.

In the present article influence of heat transfer on blood flow is analyzed in an inclined porous artery in the presence of stenosis by considering variation in viscosity. Effect of heat source parameter is duly taken care in equation of energy. Two assumptions of blood as an incompressible Newtonian biomagnetic fluid and stenosis as mild stenosis are considered. So taking care of all these assumptions and under the corresponding boundary conditions, modeling has been done for governing equations of velocity and temperature profiles. HPM method is used for solving these nonlinear differential equations [5, 9, 31]. MATLAB R2015b generated codes are used to study the effects of inclination angle of an artery(γ), porosity parameter (Z), heat source parameter(Q) and applied magnetic field parameter (M) through graphs .

2. THE MATHEMATICAL MODEL

The blood flow is assumed to be flowing in cylindrically shaped non-tapered artery in the axial direction as shown in Fig.1 it is electrically conducting in such a way that a uniform magnetic field (M) is applied perpendicular to the flow direction. Through out region of the blood flow in uniform arterial tube a non-uniform suspension viscosity is considered , which varies with packed cell volume of the red blood cells. A case of symmetrically shaped mild stenosis is considered in order to make the model in dimensionless form.

Let us Consider an incompressible magnetohydrodynamic(MHD) Newtonian fluid of density ρ and variable viscosity $\bar{\mu}$ flowing through a porous medium in a tube having finite length L . Artery with stenosis is inclined at an angle γ from the vertical axis. Consider the cylindrical coordinate system (r , θ , z)in such a way that \bar{u}, \bar{v} and \bar{w} are the velocity component in \bar{r} , $\bar{\theta}$ and \bar{z} directions respectively.

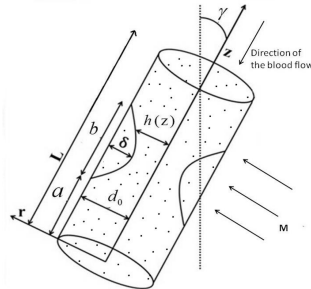


FIGURE 1. Geometry of an inclined non-tapered artery

The governing equations for the model are as follows
continuity Equation

$$(2.1) \quad \frac{\partial \bar{u}}{\partial \bar{r}} + \frac{\bar{u}}{\bar{r}} + \frac{\partial \bar{w}}{\partial \bar{z}} = 0,$$

momentum Equation (z- direction)

$$(2.2) \quad \rho \left[\bar{u} \frac{\partial \bar{u}}{\partial \bar{r}} + \bar{w} \frac{\partial \bar{u}}{\partial \bar{z}} \right] = - \frac{\partial \bar{P}}{\partial \bar{r}} + \frac{\partial}{\partial \bar{r}} \left[2\bar{\mu} \frac{\partial \bar{u}}{\partial \bar{r}} \right] + 2\frac{\bar{\mu}}{\bar{r}} \left[\frac{\partial \bar{u}}{\partial \bar{r}} - \frac{\bar{u}}{\bar{r}} \right] + \frac{\partial}{\partial \bar{z}} \left[\bar{\mu} \left(\frac{\partial \bar{u}}{\partial \bar{z}} + \frac{\partial \bar{w}}{\partial \bar{r}} \right) \right],$$

momentum Equation (r- direction)

$$(2.3) \quad \rho \left[\bar{u} \frac{\partial \bar{w}}{\partial \bar{r}} + \bar{w} \frac{\partial \bar{w}}{\partial \bar{z}} \right] = - \frac{\partial \bar{P}}{\partial \bar{z}} + \frac{\partial}{\partial \bar{z}} \left[2\bar{\mu} \frac{\partial \bar{w}}{\partial \bar{z}} \right] + \frac{1}{\bar{r}} \frac{\partial}{\partial \bar{r}} \left[\bar{\mu} \bar{r} \left(\frac{\partial \bar{u}}{\partial \bar{z}} + \frac{\partial \bar{w}}{\partial \bar{r}} \right) \right] - \sigma_1 \bar{\mu}_m^2 H_0^2 \bar{w} + \rho g \alpha (\bar{T} - \bar{T}_0) \cos \gamma - \frac{\bar{\mu} \bar{w}}{k_1},$$

Energy Equation

$$(2.4) \quad \rho c_p \left[\bar{u} \frac{\partial \bar{T}}{\partial \bar{r}} + \bar{w} \frac{\partial \bar{T}}{\partial \bar{z}} \right] = \frac{k}{\bar{r}} \frac{\partial}{\partial \bar{r}} \left(\bar{r} \frac{\partial \bar{T}}{\partial \bar{r}} \right) + \bar{\mu} \left(\frac{\partial \bar{w}}{\partial \bar{r}} \right)^2 - A(\bar{T} - \bar{T}_0),$$

where \bar{u} , \bar{v} and \bar{w} are the respective velocity component in the radial and axial directions. c_p is specific heat at constant pressure, k_t is the thermal-diffusion ratio and σ_1 is the electrical conductivity.

For variable viscosity

$$(2.5) \quad \mu(\bar{r}) = \mu_0(1 + \lambda \hbar(\bar{r})),$$

where

$$\hbar(\bar{r}) = H \left[1 - \left(\frac{\bar{r}}{d_0} \right)^m \right],$$

and $H_r = \lambda H$, in which λ is a constant having the value 2.5 and H is the maximum hematocrit at the center of an artery. Where m is the parameter that determines the exact shape of the velocity profile of blood and H_r is the hematocrit parameter.

Geometry of the stenosis located at point z with its maximum height of δ , is defined by the formula [18]

$$(2.6) \quad h(\bar{z}) = d(\bar{z})[1 - \eta(b^{n-1}(\bar{z} - a) - (\bar{z} - a)^n)],$$

when

$$a \leq \bar{z} \leq a + b \\ = d(\bar{z}), \quad \text{otherwise}$$

where $d(z)$ is the radius of the tapered artery in stenotic region

with

$$d(\bar{z}) = d_0 + \xi \bar{z},$$

In Eq.(2.6), n is the shape parameter which determines the shape of the constriction profile. Value $n = 2$ results symmetrically shaped stenosis and for non symmetric stenosis case n considers the values $n \geq 2$. d_0 is the radius of the non-tapered artery and ξ is the tapering parameter which is defined by $\xi = \tan(\phi)$, where ϕ is known as tapered angle and it considers the values $\phi < 0$, $\phi > 0$ and $\phi = 0$ for the case of converging, diverging and non tapered artery respectively [18].

In Eq.(2.6) parameter η is defined as

$$(2.7) \quad \eta = \frac{\delta^* n^{\frac{n}{n-1}}}{d_0 b^n (n-1)},$$

where δ is the maximum height of the stenosis located at

$$\bar{z} = a + \frac{b}{n^{\frac{n}{n-1}}}.$$

In order to represent the model in dimensionless form, let us introduce the non-dimensional variables as follows:

$$(2.8) \quad \begin{cases} \bar{u} = \frac{u u_0 \delta}{b}, & \bar{r} = r d_0, & \bar{z} = z b, & \bar{w} = w u_0, & \bar{h} = h d_0, \\ \bar{P} = \frac{u_0 b \mu_0 P}{d_0^2}, & R_e = \frac{\rho b u_0}{\mu_0}, & \Theta = \frac{(\bar{T} - \bar{T}_0)}{\bar{T}_0}, & P_r = \frac{\mu c_p}{k}, & E_c = \frac{u_0^2}{c_p T_0}, \\ Z = \frac{k_1}{d_0^2}, & M^2 = \frac{\sigma_1 H_0^2 d_0^2}{\mu_0}, & Q = A \frac{d_0^2}{k}, & G_r = \frac{g \alpha d_0^3 \bar{T}_0}{v^2}, \end{cases}$$

where R_e is the Reynolds number, E_c is the Eckert number, P_r is the Prandtl number and G_r is the Grashof number.

In the case of mild stenosis $\frac{\delta^*}{d_0} \ll 1$ and other two additional conditions [18]

$$(2.9) \quad \frac{Re \delta^* n^{\frac{1}{n-1}}}{b} \ll 1,$$

$$(2.10) \quad \frac{d_0 n^{\frac{1}{n-1}}}{b} \sim O(1),$$

Eqs.(2.1)-(2.4) change in the given non dimensional form

Continuity Equation

$$(2.11) \quad \frac{\partial w}{\partial z} = 0,$$

Momentum Equation (r-direction)

$$(2.12) \quad \frac{\partial P}{\partial r} = 0,$$

Momentum Equation (z-direction)

$$(2.13) \quad \frac{\partial P}{\partial z} = \left[\frac{1}{r} + H_r \left(\frac{1}{r} - (m+1)r^{m-1} \right) \right] \frac{\partial w}{\partial r} + \left[1 + H_r(1-r^m) \frac{\partial}{\partial r} \left(\frac{\partial w}{\partial r} \right) \right]$$

$$(2.14) \quad -w \left(M^2 + \frac{1}{Z} + \frac{H_r}{Z}(1-r^m) \right) + G_r \Theta \cos \gamma,$$

Energy Equation

$$(2.15) \quad \frac{1}{r} \frac{\partial}{\partial r} \left[r \frac{\partial \Theta}{\partial r} \right] + E_c P_r \left[\frac{\partial w}{\partial r} \right]^2 - Q \Theta = 0,$$

where $Br = E_c P_r$, Brinkman number (B_r) is the ratio between heat produced by viscous dissipation and heat transported by molecular conduction.

The corresponding boundary conditions are

$$(2.16) \quad \frac{\partial w}{\partial r} = 0, \quad \frac{\partial \Theta}{\partial r} = 0, \quad \text{at } r = 0,$$

$$(2.17) \quad w = 0, \quad \Theta = 0, \quad \text{at } r = h(z).$$

In which $h(z)$ is the geometry of the stenosis in non-dimensional form when radius of the artery is of unit length ($d_0 = 1$)

$$(2.18) \quad h(z) = (1 + \xi' z)[1 - \eta_1((z - l_1) - (z - l_1)^n)]$$

when

$$l_1 \leq z \leq l_1 + 1,$$

in Eq.(2.18), η_1 , δ , l_1 and ξ are defined as

$$\eta_1 = \frac{\delta n^{\frac{n}{n-1}}}{(n-1)}, \quad \delta = \frac{\delta^*}{d_0}, \quad l_1 = \frac{a}{b}, \quad \xi' = \frac{\xi b}{d_0}, \quad \xi = \tan(\phi).$$

3. SOLUTION

Now, use semi-analytical homotopy perturbation method to solve the nonlinear Eqs.(2.11)-(2.15) under the given boundary conditions by Eqs.(2.16)-(2.17). First, formulate following homotopies for velocity and temperature profiles

$$(3.1) \quad H(q, w) = q \left[L(w) + H_r \left(\frac{1}{r} - (m+1)r^{m-1} \right) \frac{\partial w}{\partial r} + H_r(1-r^m) \frac{\partial}{\partial r} \left(\frac{\partial w}{\partial r} \right) - \frac{\partial p}{\partial z} \right] \\ + (1-q)[L(w) - L(w_0)] - q \left[w \left(M^2 + \frac{1}{Z} + H_r \frac{(1-r^m)}{Z} \right) - \cos \gamma (G_r \Theta) \right],$$

where $q \in [0, 1]$ is the embedding parameter and $L(w)$ is the auxiliary linear operator, defined as

$$(3.2) \quad L(w) = \frac{1}{r} \left(\frac{\partial}{\partial r} \left(r \frac{\partial w}{\partial r} \right) \right),$$

$$(3.3) \quad H(q, \Theta) = (1 - q)[L(\Theta) - L(\Theta_0)] + q \left[L(\Theta) + E_c P_r \left(\frac{\partial w}{\partial r} \right)^2 - Q\Theta \right],$$

where

$$(3.4) \quad L(\Theta) = \frac{1}{r} \left(\frac{\partial}{\partial r} \left(r \frac{\partial \Theta}{\partial r} \right) \right),$$

The initial guesses used to solve these homotopies are given by

$$(3.5) \quad w_{10} = \frac{(r^2 - h^2)}{4} \left(M^2 + \frac{1}{Z} \right) \left(\frac{\partial p_0}{\partial z} \right),$$

$$(3.6) \quad \Theta_{10} = \frac{(r^2 - h^2)}{4}.$$

Now, the dependent variables can be decomposed as

$$(3.7) \quad w(r, q) = w_0 + qw_1 + q^2w_2 + O(q^3),$$

$$(3.8) \quad \Theta(r, q) = \Theta_0 + q\Theta_1 + q^2\Theta_2 + O(q^3).$$

Now, substitute the series expansion of above variables in Eq.(3.1) and Eq.(3.3), compare the coefficients of q^0 , q^1 and q^2 .

First by comparison the coefficient of q^0 in Eq.(3.1),

$$(3.9) \quad L(w_0) - L(w_{10}) = 0 \Rightarrow w_0 = w_{10} = \frac{(r^2 - h^2)}{4} \left(M^2 + \frac{1}{Z} \right) \left(\frac{\partial p_0}{\partial z} \right),$$

now compare the coefficient of q^1 in Eq.(3.1),

$$(3.10) \quad \begin{aligned} L(w_1) &= -L(w_0) - H_r \left(\frac{1}{r} - (m+1)r^{(m-1)} \right) \frac{\partial w_0}{\partial r} - H_r (1 - r^m) \frac{\partial}{\partial r} \left(\frac{\partial w_0}{\partial r} \right) \\ &+ w_0 \left(M^2 + \frac{1}{Z} + H_r \frac{(1 - r^m)}{Z} \right) - \cos\gamma (G_r \Theta_0) + \frac{\partial p_0}{\partial z}, \end{aligned}$$

and by compare the coefficient of q^2 in Eq.(3.1), get the equation as follows

$$(3.11) \quad \begin{aligned} L(w_2) &= -H_r \left(\frac{1}{r} - (m+1)r^{(m-1)} \right) \frac{\partial w_1}{\partial r} - H_r (1 - r^m) \frac{\partial}{\partial r} \left(\frac{\partial w_1}{\partial r} \right) \\ &+ w_1 \left(M^2 + \frac{1}{Z} + H_r \frac{(1 - r^m)}{Z} \right) - \cos\gamma (G_r \Theta_1) + \frac{\partial p_1}{\partial z}. \end{aligned}$$

Now in Eq.(3.3), compare coefficients of q^0 , q^1 and q^2 respectively

$$(3.12) \quad q^0 : \quad L(\Theta_0) - L(\Theta_{10}) = 0 \Rightarrow \Theta_0 = \Theta_{10} = \frac{(r^2 - h^2)}{4},$$

$$(3.13) \quad q^1 : \quad L(\Theta_1) = -L(\Theta_0) - E_c P_r \left(\frac{\partial w_0}{\partial r} \right)^2 + Q\Theta_0,$$

$$(3.14) \quad q^2 : \quad L(\Theta_2) = -2E_c P_r \left(\frac{\partial w_0}{\partial r} \right) \left(\frac{\partial w_1}{\partial r} \right) + Q\Theta_1.$$

So with the help of initial guesses w_{10} , Θ_{10} from Eq.(3.5) and Eq.(3.6) and by using the definition of linear operators $L(w_0)$ and $L(\Theta_0)$ from Eq.(3.2) and Eq.(3.4), in Eq.(3.10) and Eq.(3.11), get the expressions for w_1 and Θ_1 as

$$(3.15) \quad w_1 = \frac{(r^2 - h^2)}{4} \left(\frac{\partial p_0}{\partial z} \right) \left(1 - (M^2 + \frac{1}{Z}) \right) - \frac{\cos \gamma}{64} (r^4 + 3h^4 - 4r^2h^2) G_r \\ + \frac{H_r}{4Z} \left(\frac{\partial p_0}{\partial z} \right) \left(M^2 + \frac{1}{Z} \right) \left(\frac{r^4 + 3h^4}{16} + \frac{(h^{m+4} - r^{m+4})}{(m+4)^2} + \frac{h^2r^{m+2} - h^{m+4}}{(m+2)^2} \right) \\ - \frac{H_r}{4Z} \left(\frac{\partial p_0}{\partial z} \right) \left(M^2 + \frac{1}{Z} \right) \left(\frac{r^2h^2}{4} \right) + \left(\frac{\partial p_0}{\partial z} \right) \left(M^2 + \frac{1}{Z} \right)^2 \left(\frac{r^4}{16} + \frac{3h^4}{16} - \frac{h^2r^2}{4} \right) \\ - \frac{H_r}{2} \left(\frac{r^2 - h^2}{2} + \frac{h^{m+2} - r^{m+2}}{m+2} \right) \left(\frac{\partial p_0}{\partial z} \right) \left(M^2 + \frac{1}{Z} \right),$$

$$(3.16) \quad \Theta_1 = -E_c P_r \frac{(r^4 - h^4)}{64} \left(\frac{\partial p_0}{\partial z} \right)^2 \left(M^2 + \frac{1}{Z} \right)^2 - \left(\frac{r^2 - h^2}{4} \right) + Q \left(\frac{r^4}{16} + \frac{3h^4}{16} - \frac{r^2h^2}{4} \right).$$

Final expressions for w_2 and Θ_2 have been calculated by putting the values of w_1 , Θ_1 in Eq.(3.11) and Eq.(3.14) and with the help of MATLAB 2015a. We obtain full expressions for $w(r, z)$ and $\theta(r, z)$ by putting the values of w_1, w_2, θ_1 and θ_2 in Eq.(3.7) and Eq.(3.8) respectively.

4. RESULTS AND DISCUSSIONS

Matlab codes are used to evaluate the analytical results obtained for the velocity and temperature variation and the distribution of wall shear stress (τ_s) in fluid flow. In order to observe the quantitative effects of inclination angle of the artery, magnetic field parameter (M), hematocrit parameter (H_r), porosity parameter(Z), heat source parameter (Q), Brinkman number (B_r), Grashof number (G_r) and the height of the stenosis (δ) following data is used.

$d_0 = 1$, $h(z) = 0.9$, $a = 0.25$, $b = 1$, $\gamma = \frac{\pi}{6}$, $Z = 0.3$, $n = 2$, $G_r = 2$, $z = 0.5$, $\delta = 0.1$, $H_r = 1$, $M = 1.5$, $Q = 1.5$, $B_r = 2$.

4.1. Effects of Magnetic field parameter (M). Figs.2(a) and 2(b) in Fig.2, display the effect of

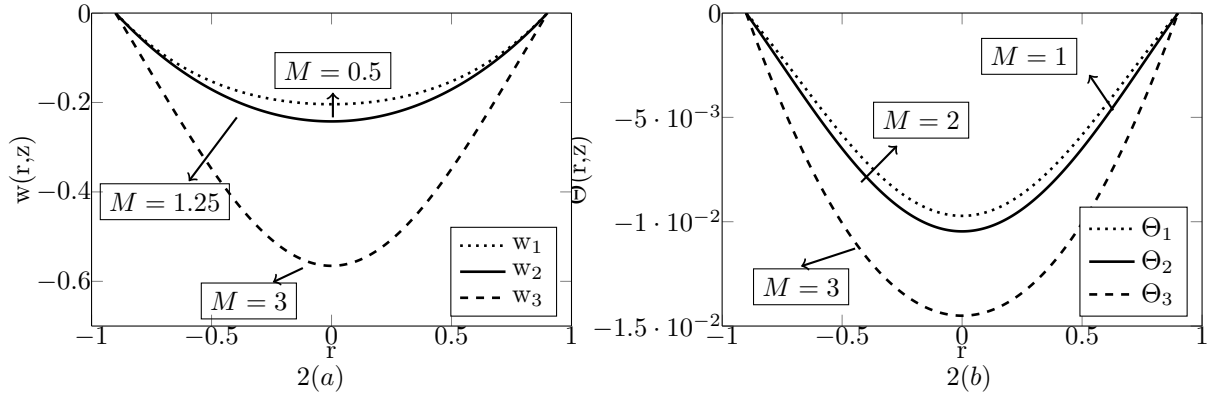


FIGURE 2. Variation with magnetic field parameter (M) at $B_r = 2$, $n = 2$, $\delta = 0.1$, $z = 0.5$, $Z = 0.3$, $G_r = 2$, $H_r = 1$, $Q = 1.5$, $\gamma = \frac{\pi}{6}$

magnetic field parameter on velocity and temperature profiles of blood respectively. It can be easily seen from Fig.2(a) that velocity decreases relatively with increasing values of magnetic field parameter. It happens because of the fact that when blood flows under the influence of magnetic field, the action of magnetization applies a rotational motion on the charged particles of the blood. The continuous rotational motion of charged particles causes red blood cells to be more suspended in blood plasma and this increases the internal viscosity of the blood. Increased viscosity affects the blood flow by increasing the value of flow resistance, this causes decrement in the value of blood velocity. Lorentz force opposes the motion of blood particles, which reduces velocity of the blood flow [34].

From Fig.2(b) it is clear that as the value of magnetic field parameter increases, temperature profile decreases. As it has been discussed above that with an increment in the value of magnetic field parameter results as increasing value of viscosity. So by physical law of viscosity, this follows in a right manner that with an increment in the value of magnetic field parameter results in the direction of decreasing value of temperature profile.

4.2. Effects of Grashof number (G_r). Fig.3(a) in Fig.3 velocity profile is plotted for different values of Grashof number. It is clear from Fig.3(a) that as the scale of the Grashof number increasingly changes from 1 to 3, velocity profile increases.

Fig.3(b) in Fig.3 displays the variation in temperature profile with Grashof number. It can be seen clearly from Fig.3(b) that, as value of the Grashof number increases, temperature profile also increases. So increase in the Grashof number is for to increase the rate of heat transfer effect at the arterial wall.

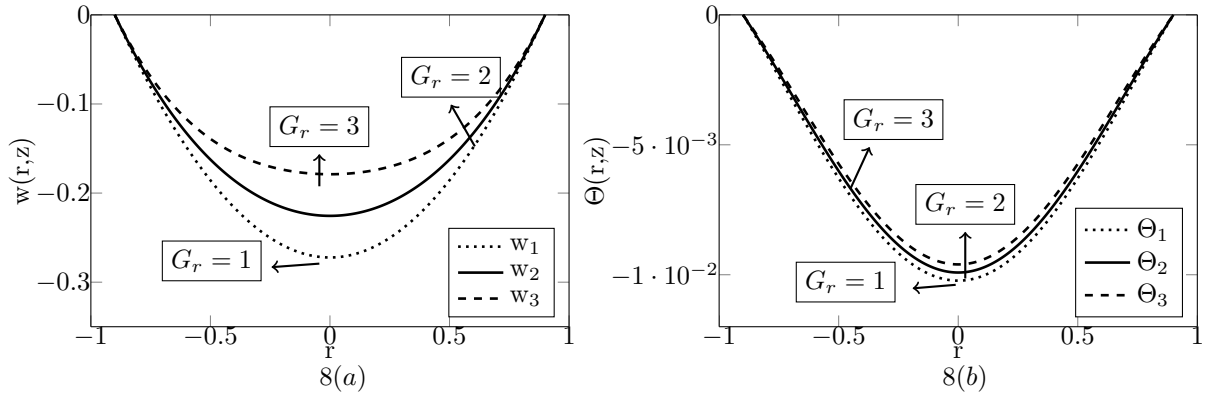


FIGURE 3. Variation in Velocity and Temperature profiles with Grashof number (G_r)

4.3. Effects of Porosity parameter (Z). Figs.4(a) and 4(b) in Fig.4 display the graphical features of porosity parameter on the profiles of velocity and temperature. It is clear from Fig.4(a) that velocity profile increases with increasing values of the porosity parameter. So in the case of porosity parameter velocity has its minimum value at middle of the artery. Velocity profile with porosity parameter shows this behavior may be because, when a fraction of the voids volume over the total volume increases, it can be more possible for fluid to move from one place to another place in the artery. Fig.4(b) marks that the temperature profile increases with increasing values of porosity parameter and it takes place may be because of viscous nature of the fluid which decreases with increasing values of velocity.

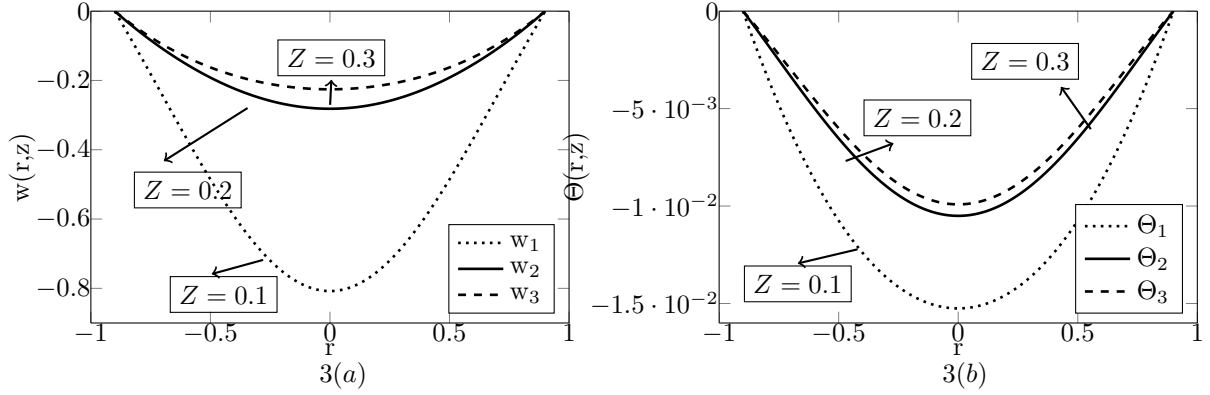
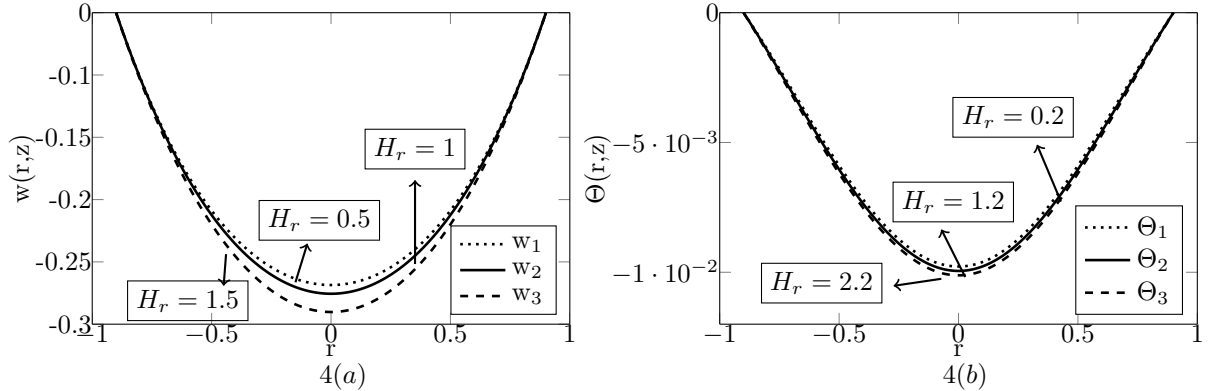


FIGURE 4. Variation in Velocity and Temperature profiles with porosity parameter

4.4. Effects of Hematocrit parameter (H_r) and Heat source parameter (Q). Figs.5(a) and 5(b) in Fig.5 illustrates the distribution of velocity and temperature profiles for different values of the hematocrit parameter H_r . Fig.5(a) shows that the velocity profile decreases with increasing values of hematocrit parameter. In blood hematocrit is the volume percentage of red blood cells, and in the artery as the number of red blood cell increases in volume, density of blood flow increases relatively. Increased density of blood slows down the flow of blood and this causes decreased velocity of the blood flow.

FIGURE 5. Variation in Velocity and Temperature profiles with Hematocrit parameter (H_r)

From Fig.5(b) it can be clearly observed that as the value of hematocrit parameter increases, temperature profile decreases and so increase in the value of H_r is to decrease the rate of heat transfer at the stationary artery wall.

Figs.6(a) and 6(b) in Fig.6 mark the variation of velocity and temperature profiles for different values of heat source parameter. It can be seen from Fig.6(a) that as the value of the heat source parameter increases, velocity of the blood flow decreases. From Fig.6(b) it is clear that as value of the heat source parameter increases, temperature profile decreases respectively. It is observed through these figures that velocity and temperature achieves its maximum value at the wall of the artery and attain minimum value at middle of the artery for heat source parameter.

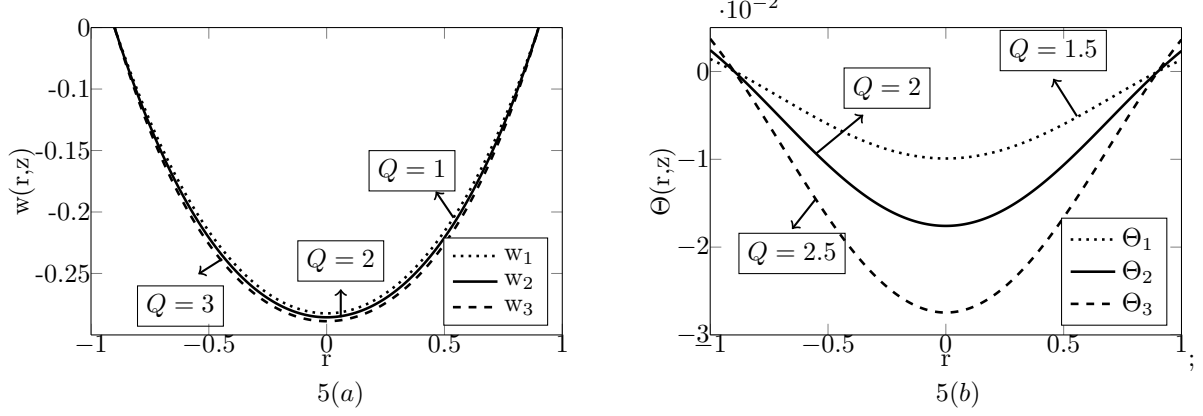


FIGURE 6. Variation in Velocity and Temperature profiles with Heat source parameter (Q)

4.5. Effects of Inclination Angle (γ) of the Artery. Figs.7(a) and 7(b) in Fig.7 illustrate the distribution of velocity and temperature profiles for different inclination angles of the artery. Fig.7(a) shows that as the angle made by the artery from vertical axes changes increasingly from 0 to $\frac{\pi}{3}$, velocity profile decreases respectively. it can be observed clearly from Fig.7(b) that as the inclination angle of the artery made by the vertical axes increases in the values from 0 to $\frac{\pi}{3}$, temperature profile decreases respectively.

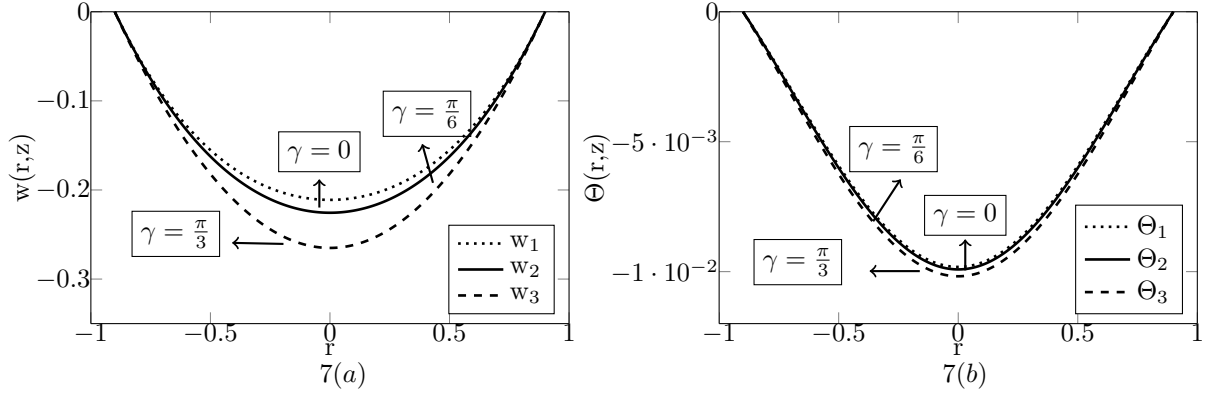


FIGURE 7. Variation in Velocity and Temperature profiles with Inclined angle of the artery (γ)

4.6. Effects of the height of the stenosis (δ). Figs.8(a) and 8(b) in Fig.8 are plotted to show the effects of height of the stenosis (δ) on velocity and temperature profiles. Fig.8(a) shows that velocity profile increases as the height of the stenosis increases and it is clear from Fig.8(b), as the height of the stenosis increases, temperature profile also increases. So from these figures it is observed that velocity and temperature profiles attain its maximum value at arterial wall and minimum value at the middle of the artery.

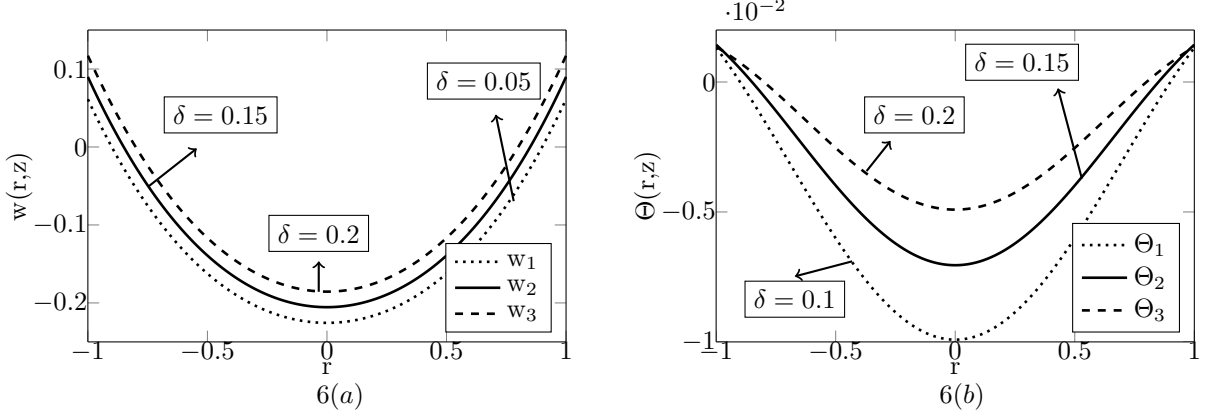


FIGURE 8. Variation in Velocity and Temperature profiles with height of the stenosis (δ)

4.7. Effects of Brinkman number (B_r). Effect of the Brinkman number on the temperature profile is depicted in Table 1. From Table 1 it is clear that as the value of Brinkman number increases, temperature profile decreases respectively and it clears that temperature profile increases respectively from middle of the artery to side wall of the artery.

Variation in temperature profile with different values of B_r			
r	$B_r = 1$	$B_r = 4$	$B_r = 7$
-0.9	-0.0045294569	-0.0045879008	-0.0046463448
-0.6	-0.0083862685	-0.0084629178	-0.0085395671
-0.3	-0.0098875358	-0.0099679781	-0.0100484205
0.3	-0.0083862685	-0.0084629178	-0.0085395671
0.6	-0.0045294569	-0.004587900	-0.004646344
0.9	-0.0045294569	-0.0045879008	-0.0046463448

TABLE 1. Variation in Temperature profile with Brinkman number

4.8. Expression for the Shear Stress. The nonzero dimensionless shear stress is given by

$$(4.1) \quad \tilde{S}_{rz} = \left(\frac{\partial w}{\partial r} \right),$$

expression for wall shear stress is

$$(4.2) \quad \tilde{S}_{rz} = \left[\frac{\partial w}{\partial r} \right]_{r=h}.$$

To find the expression for shearing stress at the stenosis throat i.e., the wall shear at the maximum height of the stenosis located at $z = \frac{a}{b} + \frac{1}{n^{\frac{1}{n-1}}}$, put $h = (1 - \delta)$. So the expression for the wall shear at the maximum height of the stenosis is given by

$$(4.3) \quad \tilde{\tau}_s = \left[\tilde{S}_{rz} \right]_{h=(1-\delta)}.$$

Figs.9(a) in Fig.9 are plotted for the wall shear stress against the axial distance (z) with different values of shape parameter(n). Fig.9(b) in Fig.9 is plotted for the wall shear stress at stenosis throat τ_s against

the height of the stenosis δ for different values of the magnetic field parameter (M). From Fig.9(b) it is clear that as values of the magnetic field parameter changes from 1.5 to 3, the wall shear stress at stenosis throat increases relatively.

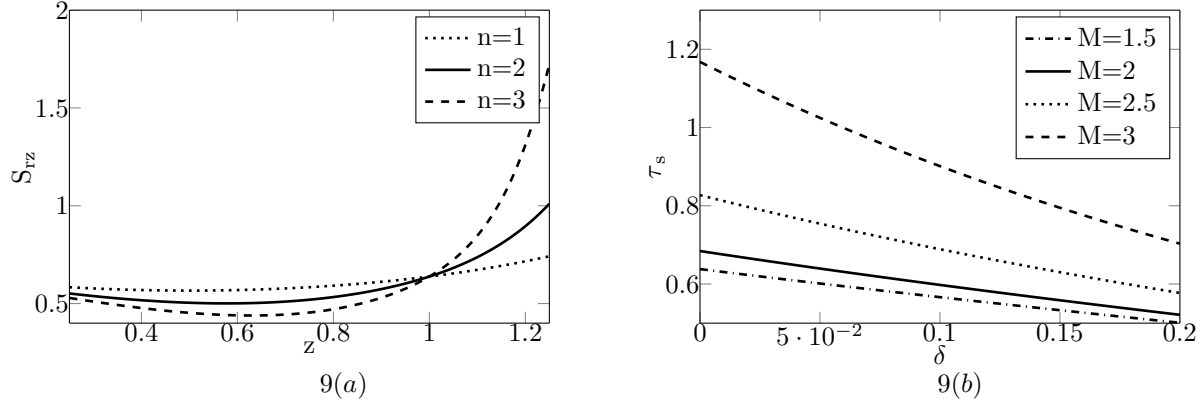


FIGURE 9. Variation of shear stress at arterial wall and stenosis throat

Figs.10(a) in Fig.10 display the effects of hematocrit parameter (H_r) on wall shear stress at stenosis throat. From Fig.10(a) it is clear that as value of hematocrit parameter increases from 0.5 to 2, wall shear stress at stenosis throat increases respectively. Fig.10(b) in Fig.10 marks the effects of porosity parameter Z on wall shear stress at stenosis throat. From Fig.10(b) it can be easily observed that as the value of porosity parameter changes increasingly from 0.1 to 0.5, wall shear stress at stenosis throat decreases relatively.

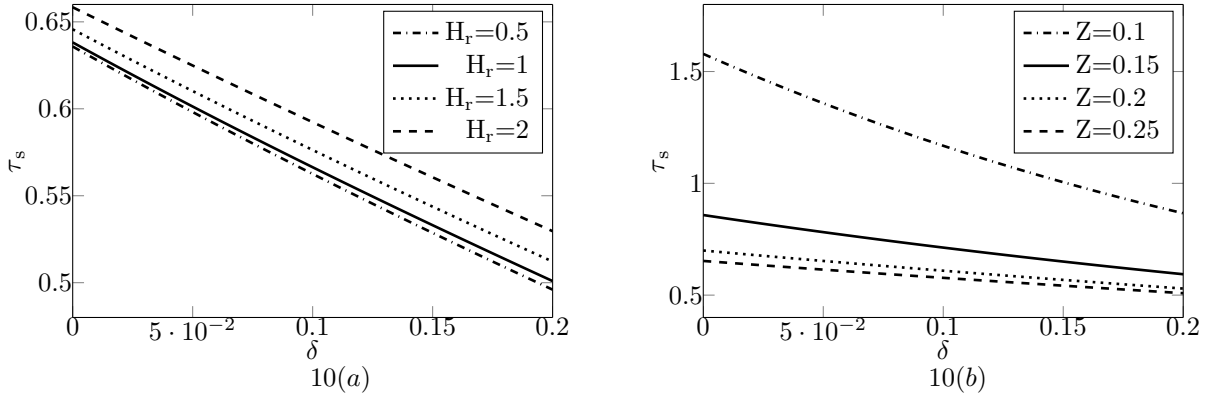


FIGURE 10. Variation of shear stress at stenosis throat

5. CONCLUSION

The magnetohydrodynamic flow and heat transfer effects in a stenosed inclined artery with hematocrit-dependent viscosity have been studied through this paper. The mathematical problem is solved analytically by using homotopy perturbation technique. The study is particularly motivated towards the flow and heat transfer phenomenon under the influence of magnetic field and external heat source. The significant findings of this paper are summarized below

- (1) Velocity and temperature profiles decrease with increasing values of magnetic field parameter (M). This happens because of the Lorentz force which opposes the motion of the blood flow in the artery.
- (2) Velocity and temperature profiles decrease as an inclined angle of the artery (γ) increases from 0 to $\frac{\pi}{3}$.
- (3) Velocity and temperature profiles decrease with increasing values of hematocrit parameter (H_r). Increasing values of hematocrit parameter increase the volume of the red blood cell in the artery. This causes blood motion to slow in the artery.
- (4) Velocity and temperature profiles increase as value of height of the stenosis (δ) increases. In this article case of mild stenosis have been considered, so values of δ vary in between range of the mild stenosis.
- (5) Velocity and temperature profiles increase with increasing values of the porosity parameter (Z).
- (6) Velocity and temperature profiles decrease with an increase in the value of the heat source parameter (Q).
- (7) With increasing values of the Grashof number (G_r) both velocity and temperature profiles increase.

NOMENCLATURE

u - Velocity in the z-direction
 v - Velocity in the r-direction
 σ_1 - Electrical conductivity
 δ - Height of the stenosis
 ξ - Tapered angle of the artery
 B_r - Brinkman number
 G_r - Grashof number
 γ - Angle of the inclined artery
 M - Magnetic field parameter
 Z - Porosity parameter
 Q - Heat source parameter
 H_r - Hematocrit Parameter
 H - Maximum hematocrit at center
 P_r - Prandtl number
 E_c - Eckert number
 R_e - Reynolds number
 μ - Viscosity
 c_p - Specific heat
 k_t - Thermal diffusion

ACKNOWLEDGEMENT

Authors are sincerely thankful to the Department of Science and Technology, Government of India (SR/FST/MSI-090/2013(C)) for their financial support.

REFERENCES

- [1] I. ABDULLAH, N. AMIN, AND T. HAYAT, *Magnetohydrodynamic effects on blood flow through an irregular stenosis*, International Journal for Numerical Methods in Fluids, 67 (2011), pp. 1624–1636.
- [2] P. AKBARZADEH, *Pulsatile magneto-hydrodynamic blood flows through porous blood vessels using a third grade non-newtonian fluids model*, Computer Methods and Programs in Biomedicine, 126 (2016), pp. 3 – 19.
- [3] D. BLUESTEIN, L. NIU, R. T. SCHOPHOERSTER, AND M. K. DEWANJEE, *Fluid mechanics of arterial stenosis: Relationship to the development of mural thrombus*, Annals of Biomedical Engineering, 25 (1997), pp. 344–356.

- [4] S. BOSE AND M. BANERJEE, *Magnetic particle capture for biomagnetic fluid flow in stenosed aortic bifurcation considering particle-fluid coupling*, Journal of Magnetism and Magnetic Materials, 385 (2015), pp. 32 – 46.
- [5] A. DEMİR, S. ERMAN, B. ÖZGÜR, AND E. KORKMAZ, *Analysis of the new homotopy perturbation method for linear and nonlinear problems*, Boundary Value Problems, 2013 (2013), pp. 1–11.
- [6] M. EL-SHAHED, *Pulsatile flow of blood through a stenosed porous medium under periodic body acceleration*, Applied Mathematics and Computation, 138 (2003), pp. 479 – 488.
- [7] I. M. ELDESOKY, *Mathematical analysis of unsteady mhd blood flow through parallel plate channel with heat source*, World Journal of Mechanics, 2 (2012).
- [8] R. ELLAHI, S. RAHMAN, AND S. NADEEM, *Blood flow of jeffrey fluid in a catherized tapered artery with the suspension of nanoparticles*, Physics Letters A, 378 (2014), pp. 2973 – 2980.
- [9] A. A. HEMEDA, *Homotopy perturbation method for solving systems of nonlinear coupled equations*, Applied Mathematical Sciences, 6 (2012), pp. 4787 – 4800.
- [10] M. IKBAL, S. CHAKRAVARTY, K. K. WONG, J. MAZUMDAR, AND P. MANDAL, *Unsteady response of non-newtonian blood flow through a stenosed artery in magnetic field*, Journal of Computational and Applied Mathematics, 230 (2009), pp. 243 – 259.
- [11] A. KUMAR, C. L. VARSHNEY, AND G. C. SHARMA, *Computational technique for flow in blood vessels with porous effects*, Applied Mathematics and Mechanics, 26 (2005), pp. 63–72.
- [12] G. LAYEK, S. MUKHOPADHYAY, AND R. S. R. GORLA, *Unsteady viscous flow with variable viscosity in a vascular tube with an overlapping constriction*, International Journal of Engineering Science, 47 (2009), pp. 649 – 659.
- [13] K. LIPSCOMB AND S. HOOTEN, *Effect of stenotic dimensions and blood flow on the hemodynamic significance of model coronary arterial stenoses*, The American Journal of Cardiology, 42 (1978), pp. 781 – 792.
- [14] O. MAKINDE AND O. ONYEJEKWE, *A numerical study of {MHD} generalized couette flow and heat transfer with variable viscosity and electrical conductivity*, Journal of Magnetism and Magnetic Materials, 323 (2011), pp. 2757 – 2763.
- [15] K. R. MALLIKARJUNA REDDY C, RAMBHUPAL REDDY B., *Mathematical model governing magnetic field effect on bio magnetic fluid flow and orientation of red blood cells*, Pacific-Asian Journal of Mathematics, 5 (2011), pp. 344–356.
- [16] M. MASSOUDI AND I. CHRISTIE, *Effects of variable viscosity and viscous dissipation on the flow of a third grade fluid in a pipe*, International Journal of Non-Linear Mechanics, 30 (1995), pp. 687 – 699.
- [17] K. S. MEKHEIMER, M. H. HAROUN, AND M. A. ELKOT, *Effects of magnetic field, porosity, and wall properties for anisotropically elastic multi-stenosis arteries on blood flow characteristics*, Applied Mathematics and Mechanics, 32 (2011), pp. 1047–1064.
- [18] K. S. MEKHEIMER AND M. A. E. KOT, *The micropolar fluid model for blood flow through a tapered artery with a stenosis*, Acta Mechanica Sinica, 24 (2008), pp. 637–644.
- [19] J. MISRA, A. SINHA, AND G. SHIT, *Mathematical modeling of blood flow in a porous vessel having double stenoses in the presence of an external magnetic field*, International Journal of BiomathematicsInt. J. Biomath., 4 (2011), pp. 207 – 225.
- [20] N. MUSTAPHA, N. AMIN, S. CHAKRAVARTY, AND P. K. MANDAL, *Unsteady magnetohydrodynamic blood flow through irregular multi-stenosed arteries*, Computers in Biology and Medicine, 39 (2009), pp. 896 – 906.
- [21] S. NADEEM AND N. S. AKBAR, *Effects of heat transfer on the peristaltic transport of {MHD} newtonian fluid with variable viscosity: Application of adomian decomposition method*, Communications in Nonlinear Science and Numerical Simulation, 14 (2009), pp. 3844 – 3855.
- [22] S. NADEEM AND N. S. AKBAR, *Effects of temperature dependent viscosity on peristaltic flow of a jeffrey-six constant fluid in a non-uniform vertical tube*, Communications in Nonlinear Science and Numerical Simulation, 15 (2010), pp. 3950 – 3964.
- [23] S. NADEEM AND N. S. AKBAR, *Influence of radially varying mhd on the peristaltic flow in an annulus with heat and mass transfer*, Journal of the Taiwan Institute of Chemical Engineers, 41 (2010), pp. 286–294.
- [24] S. NADEEM, N. S. AKBAR, T. HAYAT, AND A. A. HENDI, *Influence of heat and mass transfer on newtonian biomagnetic fluid of blood flow through a tapered porous arteries with a stenosis*, Transport in Porous Media, 91 (2011), pp. 81–100.
- [25] S. NADEEM, T. HAYAT, N. S. AKBAR, AND M. MALIK, *On the influence of heat transfer in peristalsis with variable viscosity*, International Journal of Heat and Mass Transfer, 52 (2009), pp. 4722 – 4730.
- [26] R. OLLIVIER, D. BOULMIER, D. VEILLARD, G. LEURENT, S. MOCK, M. BEOSSA, AND H. L. BRETON, *Frequency and predictors of renal artery stenosis in patients with coronary artery disease*, Cardiovascular Revascularization Medicine, 10 (2009), pp. 23 – 29.
- [27] A. PANTOKRATORAS, *The falkner-Skan flow with constant wall temperature and variable viscosity*, International Journal of Thermal Sciences, 45 (2006), pp. 378 – 389.
- [28] J. S. PETROFSKY, G. BAINS, C. RAJU, E. LOHMAN, L. BERK, M. PROWSE, S. GUNDA, P. MADANI, AND J. BATT, *The effect of the moisture content of a local heat source on the blood flow response of the skin*, Archives of Dermatological Research, 301 (2009), pp. 581–585.
- [29] O. PRAKASH, S. P. SINGH, D. KUMAR, AND Y. K. DWIVEDI, *A study of effects of heat source on mhd blood flow through bifurcated arteries*, AIP Advances, 1 (2011).

- [30] M. G. RABBY, A. RAZZAK, AND M. M. MOLLA, *Pulsatile non-newtonian blood flow through a model of arterial stenosis*, Procedia Engineering, 56 (2013), pp. 225 – 231. 5th {BSME} International Conference on Thermal Engineering.
- [31] A. ROOZI, E. ALIBEIKI, S. HOSSEINI, S. SHAFIOF, AND M. EBRAHIMI, *Homotopy perturbation method for special nonlinear partial differential equations*, Journal of King Saud University - Science, 23 (2011), pp. 99 – 103.
- [32] O. A. SALOMONE, P. M. ELLIOTT, R. C. NO, D. HOLT, AND J. C. KASKI, *Plasma immunoreactive endothelin concentration correlates with severity of coronary artery disease in patients with stable angina pectoris and normal ventricular function*, Journal of the American College of Cardiology, 28 (1996), pp. 14 – 19.
- [33] B. K. SHARMA, A. MISHRA, AND S. GUPTA, *Heat and mass transfer in magneto-biofluid flow through a non-darcian porous medium with joule effect*, Journal of Engineering Physics and Thermophysics, 86 (2013), pp. 766–774.
- [34] S. SHARMA, U. SINGH, AND V. KATIYAR, *Magnetic field effect on flow parameters of blood along with magnetic particles in a cylindrical tube*, Journal of Magnetism and Magnetic Materials, 377 (2015), pp. 395 – 401.
- [35] G. SHIT AND S. MAJEE, *Pulsatile flow of blood and heat transfer with variable viscosity under magnetic and vibration environment*, Journal of Magnetism and Magnetic Materials, 388 (2015), pp. 106 – 115.
- [36] A. SINHA AND J. MISRA, *Mhd flow of blood through a dually stenosed artery: viscosity variation, variable hematocrit and velocity-slip*, The Canadian Journal of Chemical Engineering, 92 (2014), pp. 23–31.
- [37] E. TZIRTZILAKIS, *Biomagnetic fluid flow in a channel with stenosis*, Physica D: Nonlinear Phenomena, 237 (2008), pp. 66 – 81.
- [38] J. UMAVATHI, M. SHEREMET, AND S. MOHIUDDIN, *Combined effect of variable viscosity and thermal conductivity on mixed convection flow of a viscous fluid in a vertical channel in the presence of first order chemical reaction*, European Journal of Mechanics - B/Fluids, (2016).

DEPARTMENT OF MATHEMATICS, BITS PILANI (PILANI CAMPUS), PILANI, RAJASTHAN 333031, INDIA

E-mail address, B. Tripathi: bhavya.tripathi@pilani.bits-pilani.ac.in

E-mail address, B. K. Sharma: bksharma@pilani.bits-pilani.ac.in

URL, B. K. Sharma: <http://universe.bits-pilani.ac.in/pilani/bksharma/profile>